

• **Electronic Supplementary Information**

Employing T-shirt template and variant of Schweizer's reagent for constructing low-weight, flexible, hierarchically porous and textile-structured copper current collector for dendrite-suppressed Li metal

*Ruijie Zhu,^a Nan Sheng,^b Zhonghao Rao,^b Chunyu Zhu,^{a,b} * Yoshitaka Aoki,^a Hiroki Habazaki^a*

^a Graduate School of Chemical Science and Engineering & Faculty of Engineering, Hokkaido University, Sapporo 060-8628, Japan.

^b Jiangsu Province Engineering Laboratory of High Efficient Energy Storage Technology and Equipments & School of Electrical and Power Engineering; China University of Mining and Technology, Xuzhou, 221116, China

E-mail: chunyu6zhu@eng.hokudai.ac.jp (Chunyu Zhu)

Table S1. Comparison of the properties of different Cu current collectors.

Scaffold	Weight (mg)	Area (mm ²)	Thickness (mm)	Density (g cm ⁻³)
TsCu	24.4	78.5	0.55	0.565
TsCuNW	20.3	78.5	0.52	0.497
Cu foil	18.6	78.5	0.03	7.899
Cu Foam	89.8	78.5	1.21	0.945

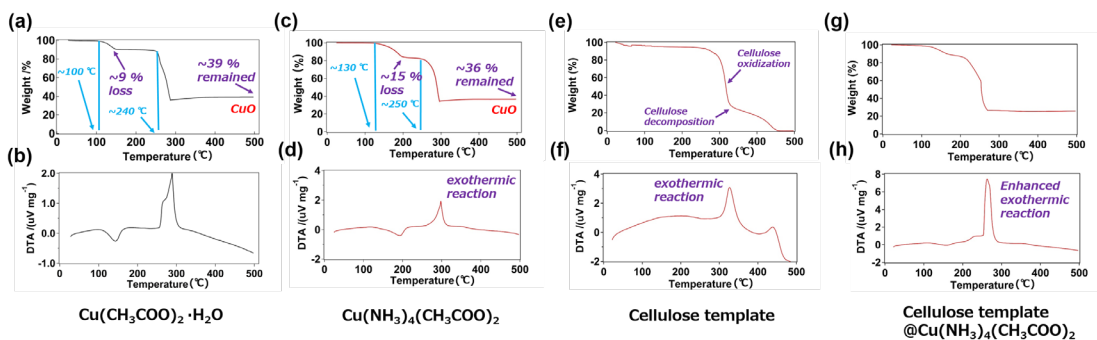


Fig. S1 TG-DTA analysis of the oxidation of (a, b) the raw material of $\text{Cu}(\text{CH}_3\text{COO})_2 \cdot \text{H}_2\text{O}$; (c, d) the precipitated copper source $\text{Cu}(\text{NH}_3)_4(\text{CH}_3\text{COO})_2$; (e, f) the T-shirt cellulose template and (g, h) the $\text{Cu}(\text{NH}_3)_4(\text{CH}_3\text{COO})_2$ coated cellulose template.

TG-DTA analysis is used for investigating the calcination behaviour of the precursors. The main ingredient of the variant Schweizer's reagent is derived from the following reaction:



The as-prepared $\text{Cu}(\text{NH}_3)_4(\text{CH}_3\text{COO})_2$ crystal, which was obtained by removing water under evaporation, shows a regular geometry with the deep blue colour (Fig. S2). As shown in Fig. S1a, the first weight loss at $\sim 100^\circ\text{C}$ corresponds to the removal of the crystal water in $\text{Cu}(\text{CH}_3\text{COO})_2 \cdot \text{H}_2\text{O}$. The oxidation of the sample begins at $\sim 240^\circ\text{C}$, which is accompanied by an exothermic reaction (Fig. S1b), due to the burning of released small carbonaceous molecules.¹ As for the calcination TG curve of $\text{Cu}(\text{NH}_3)_4(\text{CH}_3\text{COO})_2$ which is shown in Fig. S1c, the first weight loss platform occurs at $\sim 130^\circ\text{C}$, mainly due to the release of NH_3 and the removal of water. The weight loss from 250°C to 290°C corresponds to the complete decomposition and oxidation of the substance, which is also an exothermic reaction (Fig. S1d). The exothermic decomposition of $\text{Cu}(\text{NH}_3)_4(\text{CH}_3\text{COO})_2$ is different from the decomposition process of conventional $\text{Cu}(\text{OH})_2$ -based Schweizer's reagent.² The coupled exothermic reactions of cellulose oxidation (Fig. S1e) and $\text{Cu}(\text{NH}_3)_4(\text{CH}_3\text{COO})_2$ decomposition result in an enhanced exothermic reaction (Fig. S1h), which can rapidly burn off the cellulose template to in-situ form cotton-templated CuO. The morphologies of TsCuO precursor can be seen in Fig. S7, in which the CuO nano-crumbs are uniformly and tightly sintered, constructing to a firm and entire CuO framework.

It is also worth mentioning that employing copper nitrate as the metallic raw material to coat cellulose template is also possible, but due to the violent exothermic reactions and gas emission of the nitrate-enhanced oxidation reaction,³ it is difficult to maintain the textile structure.

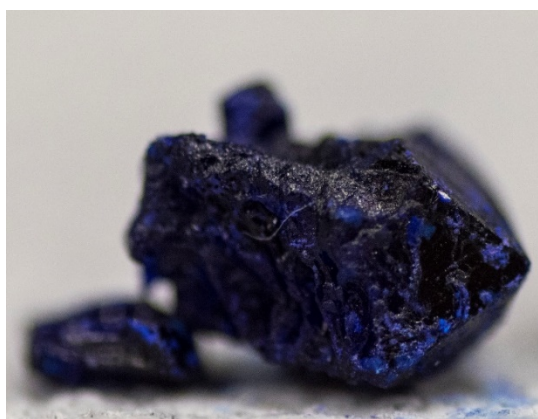


Fig. S2 Optical photo of a lump of the precipitated $\text{Cu}(\text{NH}_3)_4(\text{CH}_3\text{COO})_2$ crystal after the evaporation of water for the solution.

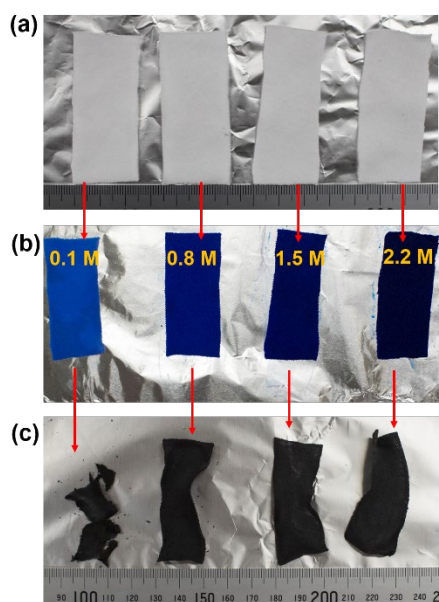


Fig. S3 Optical photos of the (a) pristine T-shirt cotton cloth template, (b) T-shirt coated by the variant Schweizer's reagent with different concentrations and (c) the obtained TsCuO after calcination in air.

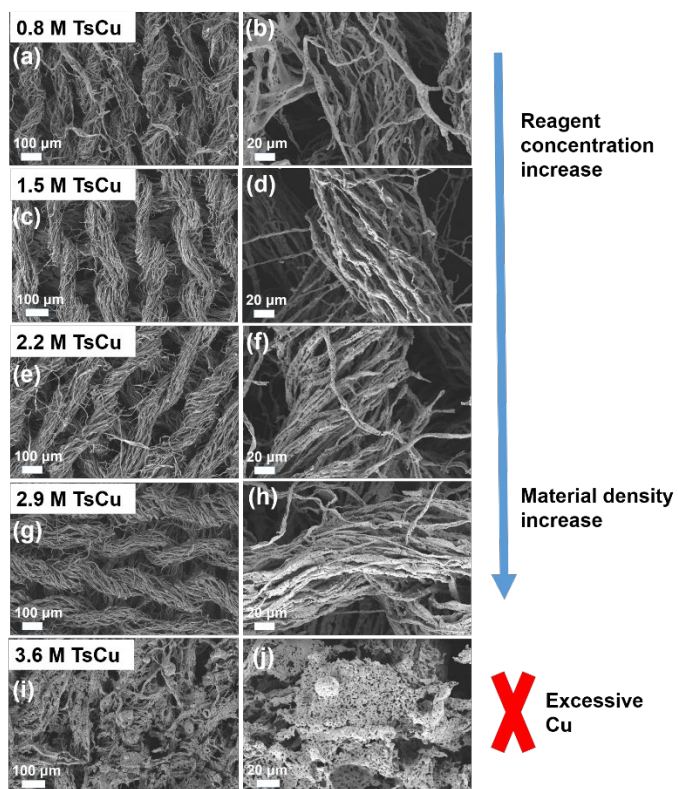


Fig. S4 SEM images for the TsCu obtained under different variant Schweizer's reagent concentrations: (a, b) 0.8 M, (c, d) 1.5 M, (e, f) 2.2 M, (g, h) 2.9 M and (i, j) 3.6 M.

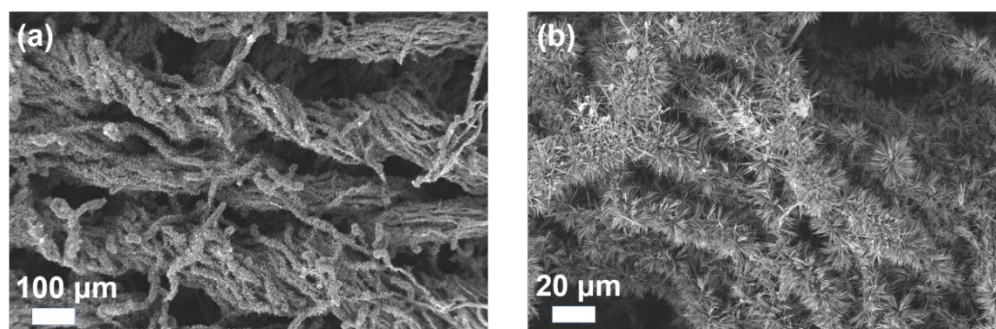


Fig. S5 SEM images of the TsCu after treatment in alkaline $(\text{NH}_4)_2\text{S}_2\text{O}_8$ solution. $\text{Cu}(\text{OH})_2$ nanowires are uniformly aligned on each Cu fiber and covered the surface of Cu substrate.

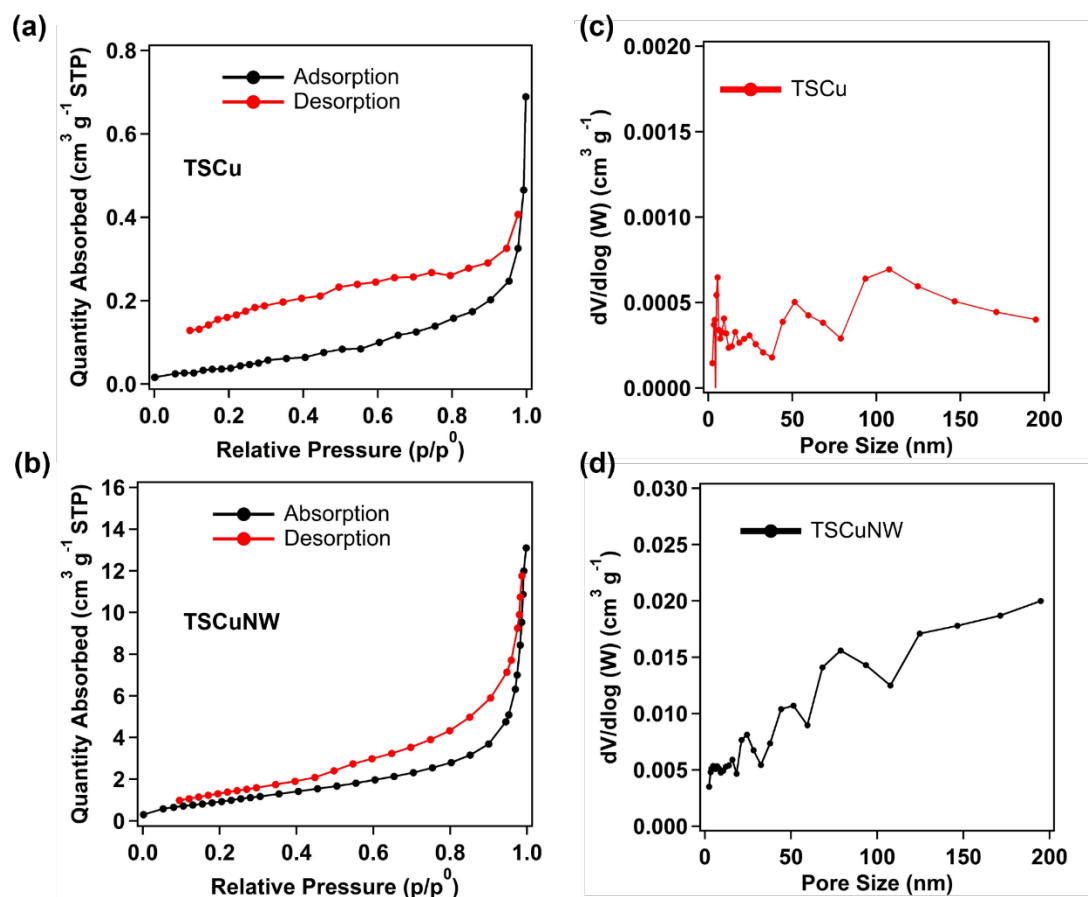


Fig. S6 Nitrogen absorption isotherms for (a) TsCu and (c) TsCuNW. BJH pore size distribution of (b) TsCu and (d) TsCuNW. The BET specific surface areas of TsCu and TsCuNW are $0.201 \text{ m}^2 \text{ g}^{-1}$ and $3.958 \text{ m}^2 \text{ g}^{-1}$, respectively. The BJH results showed that both the TsCu and TsCuNW owned nano-porous structure.

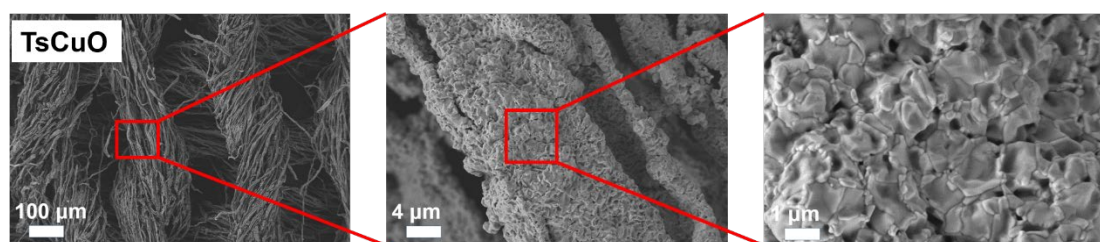


Fig. S7 SEM images of the TsCuO.

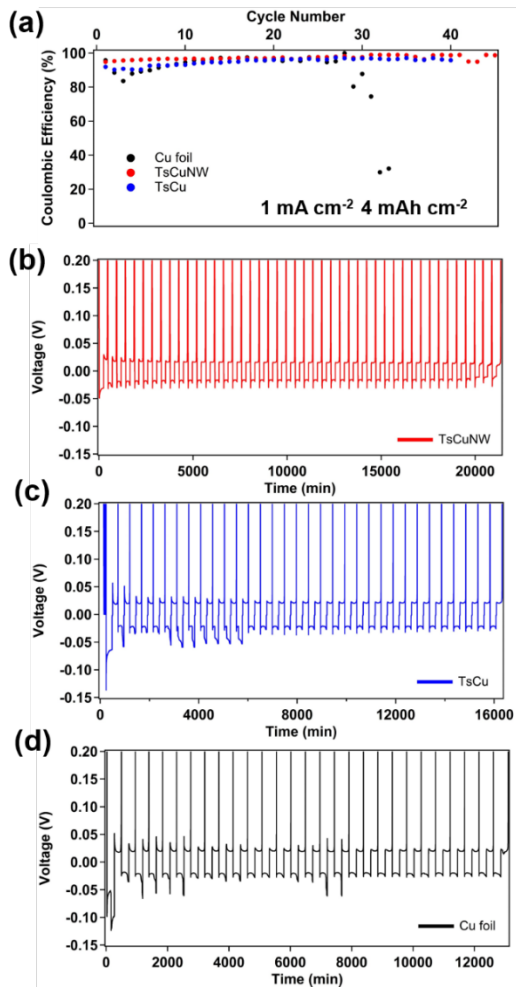


Fig. S8 (a) Coulombic efficiencies of Li plating/stripping on planar Cu foil current collector (black), the TsCuNW current collector (red) and the TsCu current collector (blue) at (a) 1 mA cm^{-2} with a capacity of 4 mA h cm^{-2} . The voltage-time curves of (b-d).

When cells are cycled at a current density of 1 mA cm^{-2} with a capacity of 4 mAh cm^{-2} , the TsCuNW still delivers a CE of 97% and a longer lifespan than both the TsCu and Cu foil. Voltage profiles during Li plating point out that the TsCuNW has better capacity for accommodating Li, due to that the over-potential during Li plating onto TsCuNW is low and stable. The cells quickly shows a failure configuration of short circuit, which is mainly due to the use of planar Li foil as the counter electrode.^{4,5}

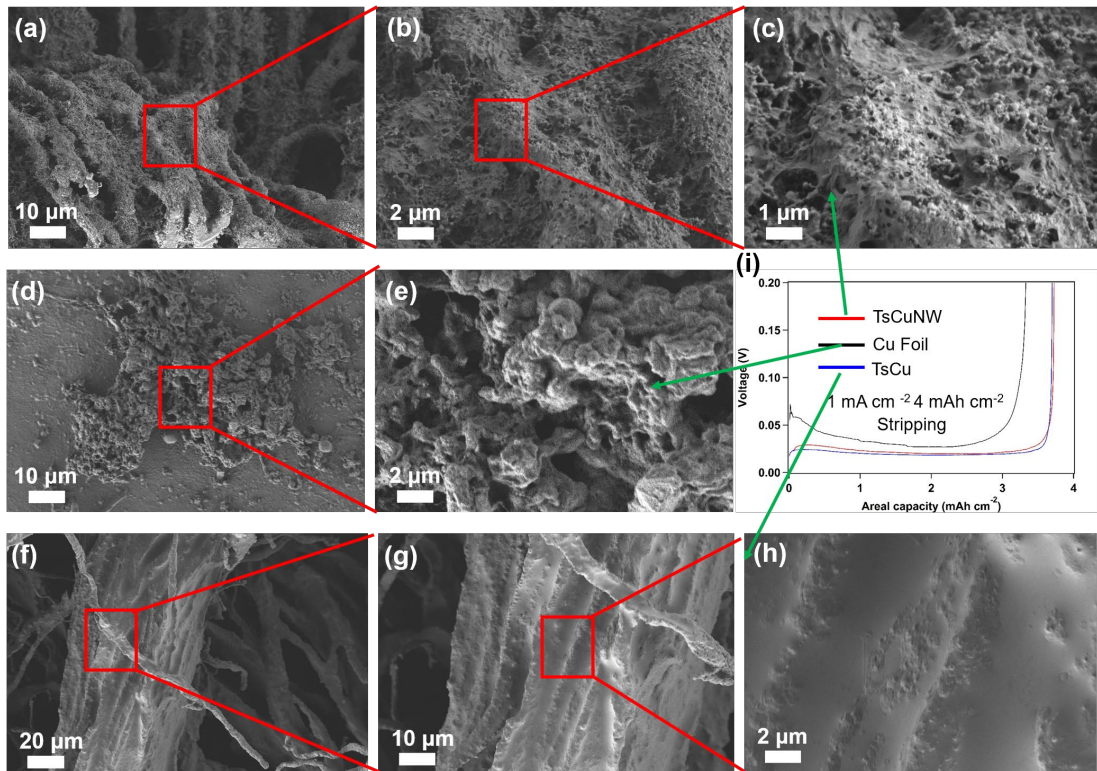


Fig. S9 Morphology observation of different Cu current collectors after stripping, which were previously plated/stripped with a controlled capacity of 4 mAh cm^{-2} : (a-c) TsCuNW; (d, e) Cu foil and (f-h) TsCu. (i) Voltage profiles for TsCuNW (red) Cu foil (Black) and TsCu (Blue) during the Li stripping process. Note that the cut-off voltage for Li stripping is 1 V.

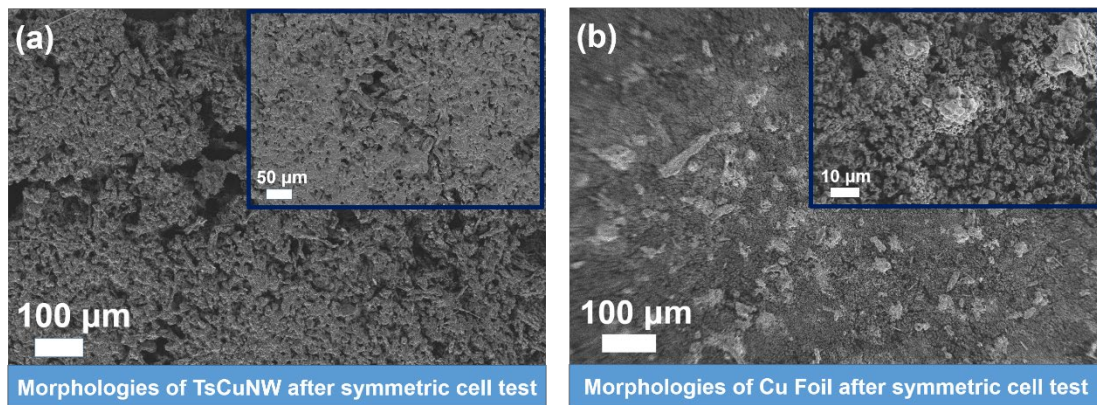


Fig. S10 SEM images of (a) Li@TsCuNW composite electrode and (b) Li@Cu foil composite electrode obtained after symmetric cell test corresponding to Fig. 6.

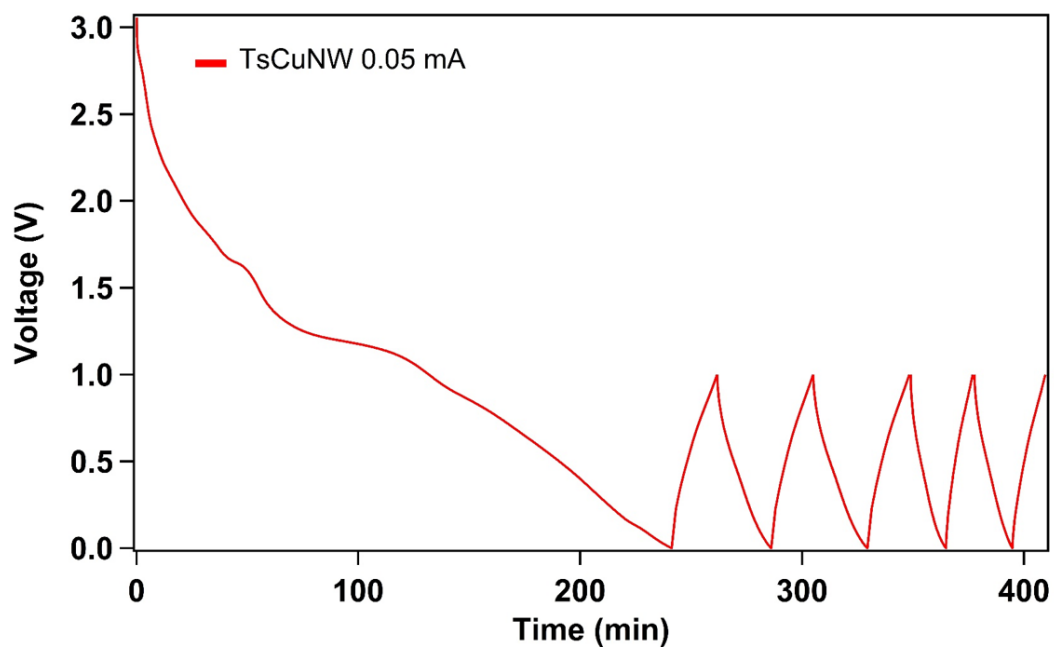


Fig. S11 Voltage profiles of the cell using TsCuNW cycled at 0-1 V (vs Li) for 6 cycles before Li plating/stripping. This process is employed to generate and stabilize the SEI.

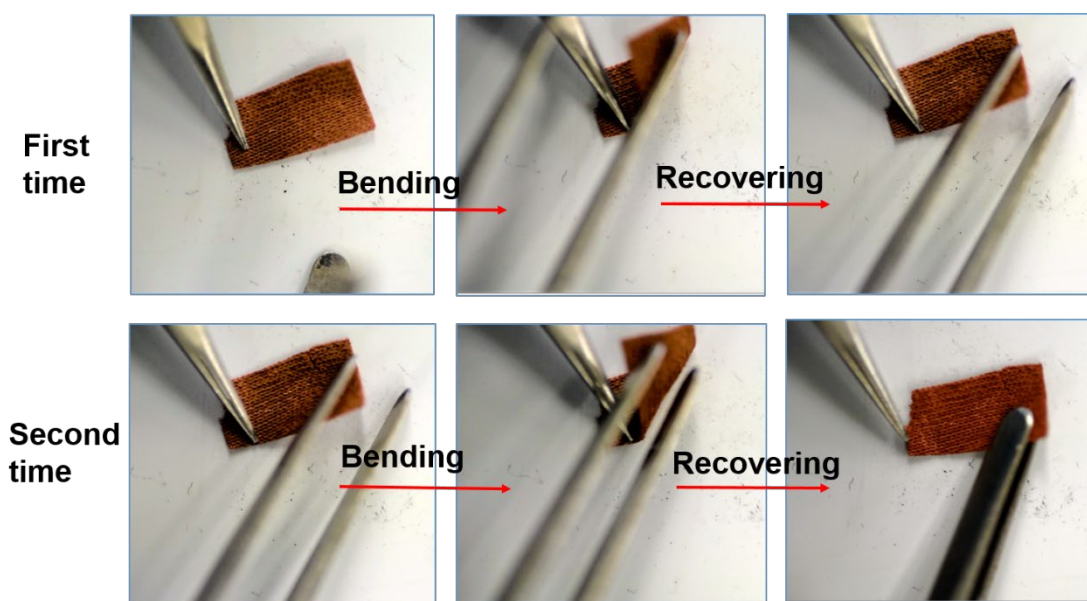


Fig. S12 Optical photographs for showing the mechanical strength and flexibility of TsCuNW. The TsCuNW can be bended and folded for many times, after which the TsCuNW can maintain the original structure.

Table S2. Mass density, surface area and cycle performance of different metallic current collectors.

Scaffold	Physical Parameters		Half Cell			Ref
	Mass density*	SSA**	Current Density Capacity	Coulombic Efficiency	Cycles	
M400 Cu mesh	3.179 g cm ⁻³	-	0.5 mA cm ⁻² 1 mAh cm ⁻²	93.8~97%	100	6
3D Porous Cu Dealloying 12 h	-	~0.5 m ² g ⁻¹	1 mA cm ⁻² 1 mAh cm ⁻²	97%	80 / 150	7
3D Cu	-	1.43 m ² g ⁻¹	1 mA cm ⁻² 1 mAh cm ⁻²	97.9%	140	8
3D Cu foil	4.181 g cm ⁻³	0.23 m ² g ⁻¹	0.5 mA cm ⁻² 1 mAh cm ⁻²	71~98.5%	50	9
Ni foam	-	-	1 mA cm ⁻² 1 mAh cm ⁻²	~90%	100	10
TsCuNW	0.497 g cm⁻³	3.96 m² g⁻¹	1 mA cm⁻² 2 mAh cm⁻²	97%	150	This work

* The mass densities of different scaffolds are calculated by the parameters that were offered in the relative supporting information.

** SSA is the abbreviation of specific surface area.

Reference

- Z. Lin, D. Han and S. Li, *Journal of Thermal Analysis and Calorimetry*, 2011, **107**, 471-475.
- Haruhiko Tanaka and T. Sadamoto, *Thermochimica Acta*, 1982, **54**, 7.
- C. Zhu, M. Takata, Y. Aoki and H. Habazaki, *Chemical Engineering Journal*, 2018, **350**, 278-289.
- P. Shi, X. B. Cheng, T. Li, R. Zhang, H. Liu, C. Yan, X. Q. Zhang, J. Q. Huang and Q. Zhang, *Advanced Materials*, 2019, DOI: 10.1002/adma.201902785.
- D. Lu, Y. Shao, T. Lozano, W. D. Bennett, G. L. Graff, B. Polzin, J. Zhang, M. H. Engelhard, N. T. Saenz, W. A. Henderson, P. Bhattacharya, J. Liu and J. Xiao, *Advanced Energy Materials*, 2015, **5**, 1400993.
- Q. Li, S. Zhu and Y. Lu, *Adv. Funct. Mater.*, 2017, **27**, 1606422.
- Q. Yun, Y. B. He, W. Lv, Y. Zhao, B. Li, F. Kang and Q. H. Yang, *Adv. Mater.*, 2016, **28**, 6932-6939.
- H. Zhao, D. Lei, Y.-B. He, Y. Yuan, Q. Yun, B. Ni, W. Lv, B. Li, Q.-H. Yang, F. Kang and J. Lu, *Adv. Energy Mater.*, 2018, **1800266**.
- C. P. Yang, Y. X. Yin, S. F. Zhang, N. W. Li and Y. G. Guo, *Nat. Commun.*, 2015, **6**, 8058.
- S.-S. Chi, Y. Liu, W.-L. Song, L.-Z. Fan and Q. Zhang, *Adv. Funct. Mater.*, 2017, **27**, 1700348.